J. At. Mol. Sci.
doi: 10.4208/jams.310810.200910a

Vol. **2**, No. 1, pp. 10-19
February 2011

Thermoelastic properties of nickel from molecular dynamic simulations

Fen Luo[a], Xiang-Rong Chen[a,b,*], Ling-Cang Cai[c], and Qiang Wu[c]

[a]*College of Physical Science and Technology, Sichuan University, Chengdu 610064, China*
[b]*International Centre for Materials Physics, Chinese Academy of Sciences, Shenyang 110016, China*
[c]*Laboratory for Shock Wave and Detonation Physics Research, Institute of Fluid Physics, Chinese Academy of Engineering Physics, Mianyang 621900, China*

Received 31 August 2010; Accepted (in revised version) 20 September 2010
Published online 17 January 2011

Abstract. The structures and elastic constants of face-centered-cubic (fcc) structured nickel at high temperature have been calculated for the first time using molecular dynamics (MD) with the direct method and the quantum Sutton-Chen (Q-SC) potential. The obtained thermoelastic constants are in excellent agreement with the experiment data. Calculated results for the radial distribution function show that the short-range atomic order of low-T is similar to the high-T solid with the applied temperatures. The thermoelastic constants, the bulk and shear modulus as a function of the applied temperature are presented. An analysis for the calculated parameters has been made to reveal mechanical stability of nickel up to 1300 K.

PACS: 46.25.Hf, 02.70.Ns

Key words: elastic properties, molecular dynamics, nickel

1 Introduction

Nickel, a d-band transition metal, is very important materials owing to broadly industrial applications such as catalysis, rechargeable batteries, and so on [1–3]. As an important transition metal in the field of condensed matter physics, it has recently attracted tremendous experimental and theoretical interest in its wide range of properties including the equation of state (EOS) [4], the elastic [5–7], transport properties [8–10], and melting properties [11–15], etc.

*Corresponding author. *Email address:* x.r.chen@tom.com (X. R. Chen)

Knowledge of thermoelastic constants is fundamental for describing the mechanical properties response of a material to applied sound velocity, anisotropy, thermoelastic stress, load deflection, fracture toughness, etc, so a complete set of single-crystal thermoelastic properties as a function of temperature is desirable. To date, several theoretical methods are applied to calculate the elastic constants, such as the tight-binding method (TB) [6], the $ab\ initio$ density-functional theory method (DFT) [7, 16], the full-potential linear muffin-tin orbital method (FP-LMTO) [17–19], and the molecular dynamic (MD) simulation methods [20–27]. For the fcc structured nickel, the theoretical investigations of elastic properties have been performed [6,7]. For example, Papanicolaou *et al.* [6] applied the tight-binding method (TB) and obtained the elastic constant, but C_{11} and C_{12} are relatively larger than experimental data [5].

In this work, we focus on the temperature dependence of elastic constants of the fcc structured Ni from MD simulation, in which the intramolecular forces are modeled by using the quantum Sutton-Chen (Q-SC) potential [28]. The validated of the Q-SC potential is confirmed by reproducing the density, cohesive energy, bulk modulus, surface energy, etc. In Section 2, the computational parameters for calculation will be presented in detail. In the following section, the theoretical result of the thermoelastic properties are listed and discussed. Finally, conclusions are summarized in Section 4.

2 Theoretical methods

In this work, we have adopted the quantum Sutton-Chen (Q-SC) potential as the reference potential. In the Q-SC potential [28], the total potential energy of the metal is given as follows

$$U_{tot}=\sum_i U_i=\sum_i \varepsilon\left(\sum_{j\neq i}\frac{1}{2}V(r_{ij})-c\sqrt{\rho_i}\right), \tag{1}$$

where $V(r_{ij})$ is a pair potential defined by the following form

$$V(r_{ij})=\left(\frac{a}{r_{ij}}\right)^n, \tag{2}$$

which accounts for a two body repulsive interaction between the atoms i and j, ρ_i is a local density representing the cohesion associated with atom i defined by

$$\rho_i=\sum_{j\neq i}\phi(r_{ij})=\sum_{j\neq i}\left(\frac{a}{r_{ij}}\right)^m. \tag{3}$$

In Eqs. (1)-(3), ε sets the overall energy scale, r_{ij} is the distance between the atom i and j, a is an arbitrary length parameter leading to dimensionless for $V(r_{ij})$ and ρ_i, c_i is a dimensionless parameter scaling the attractive term relative to the repulsive term, n and m are positive integer parameters such that $n>m$. The fitted parameters for Ni [28] are $n=10$, $m=5$, $\varepsilon=0.0073767$ eV, $c=84.745$ and $a=3.5157$ Å.

We performed MD simulations of a super cell consisted of $5\times5\times5$ conventional unit cell (500 Ni atoms), which is sufficient for the statistics of the equilibrium properties, such as pressure, temperature, energy, etc. In simulations, the NVT ensemble [29] were applied to reach the constant volume and temperature. The potential cutoff radius of 8 Å was used and the smooth particle mesh Ewald method [30] was employed with electrostatic interaction. Integration of the equation of motion has been performed with a time step of 1 fs; the system was equilibrated for a minimum of 6000 fs (6000 time steps), and statistical average of properties such as volumes and energies were computed over the remaining time of the 4000 fs (4000 time steps) simulation. We have used these relatively long simulation runs to ensure that the elastic constants extracted from the MD runs are converged. All the calculations are implemented by the DL_POLY2.17 program [31].

The elastic constants can be calculated from MD simulations using the strain- fluctuation method [20], stress-fluctuation method [21–23], and direct method [24]. The strain- fluctuation method converges slowly, while the stress-fluctuation method involves interatomic potential derivative terms that must be evaluated in the MD simulations. Herein, we used the direct method of Gao *et al.* [25, 26] based on the correlation between the stress and strain. Our practical procedure for the elastic constants calculations is as follows.

First, we construct an orthorhombic simulation cell, whose edge vectors are parallel with the edges of the conventional unit cell of nickel lattice, with [100] along x, [010] along y, [001] along z. Then, to obtain the C_{11} and C_{12}, we should scale x direction by a factor $1+e$, where e is deformation ratio ranging from -0.005 to 0.005 with 0.001 interval. For the small value of e the system is under a strain $\varepsilon_{xx}=|e|$. From the Hooke's law, we have [25, 26]

$$\sigma_{xx}=C_{11}|e|, \tag{4}$$

$$\sigma_{yy}+\sigma_{zz}=2C_{12}|e|. \tag{5}$$

In the NVT simulations, the corresponding stresses, σ_{xx}, σ_{yy} and σ_{zz} can be found from the ensemble averages and C_{11} and C_{12} can be calculated with Eqs. (4) and (5).

To determine C_{44}, we construct an orthorhombic simulation cell, whose one edge is parallel with the [110] direction of conventional unit cell. If a strain of $1+e$ is applied along the [110] direction, then the pressure an imaginary plane perpendicular to the [110] direction P_{110} can be calculated by [25, 26]

$$P_{110}=\frac{1}{2}(C_{11}+C_{12}+2C_{44})|e|. \tag{6}$$

The pressure P_{110} can be obtained from the NVT simulation.

Finally, the three elastic constants of the fcc crystal can be calculated from the direct method described above.

3 Results and discussion

The canonical NVT ensemble is applied to the simulations of the direct method. The dependence must be determined to ensure that all simulations are done at zero pressure owing

to the lattice of nickel is dependence upon temperature. So a series of MD simulation with NPT ensemble [32] were conducted. Through these calculations, we can obtain the equilibrium lattice parameters. The equilibrium lattice constants of fcc Ni from present calculation is $a=3.510$ Å is well according with the experiment data of 3.523 Å [33] at ambient condition. The isothermal compression curves compared with experiment [4] is shown in Fig. 1, in which the 300 K isotherm is in excellent agreement with experiment values at low pressure, but a little deviate from experiment at high pressure. The influence of temperature on volume is much smaller than that of the pressure on the volume. At zero pressure, when the temperature increases from 300 K to 1500 K, the volume increase about 2%. However, the volume just decreases 13% with the increasing of temperature from 0 to 300 GPa. We show the isobars at different pressures versus temperature in Fig. 2. When temperature goes from 300 K to 1500 K at 0 GPa, the calculated volume expands about 6.6%. Under high pressure, the thermal expansion is suppressed quickly by pressure.

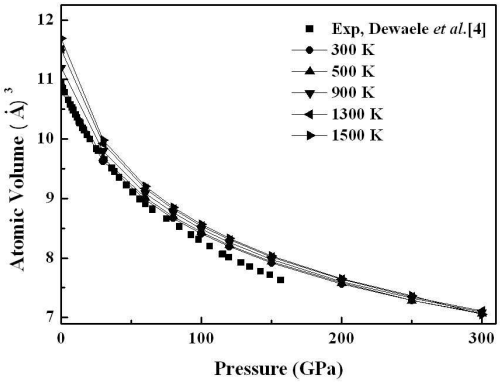

Figure 1: Isotherms of the fcc Ni at various temperatures compare with the experiment result [4].

In order to investigate the behaviour of fcc structured of nickel at high temperature, we have run the MD simulation at a number of temperatures ranging from 300 K to 1500 K at zero pressure. Fig. 3 reports our calculated radial distribution function $g(r)$ at $T=300$ K, 900 K, 1500 K. At 300 K, the shells containing 12 first neighbors and 6 second neighbors at interatomic radius of $r=2.48$ Å and $r=3.52$ Å are clearly separated, and between the second and the third shells $g(r)$ goes to zero at $r\approx 3.03$ Å. However, at 900 K, the third and higher neighbors becoming broadened, while the similar trends of $g(r)$ are showed at 1500 K. Except that, we can found the third and fourth atomic shells moves uptowns from zero. We define the coordination number N_c in the usual way as $N_c=4\pi\bar{\rho}\int_0^{r_c} g(r)r^2dr$, which $\bar{\rho}$ is the bulk number density and r_c is the distance of first minimum. The r_c of the three temperatures are 3.03, 3.14, and 3.19 Å and the corresponding coordination number N_c are 12, 12 and 12, which shows the coordination number is unchanged in the three temperatures.

With the direct method, the strain-stress relationships were applied to obtain the elastic constant in NVT ensemble. Fig. 4 shows the typical linear dependence of σ_{xx}, $\sigma_{yy}+\sigma_{zz}$, P_{110} on the compassion ratio e. Then, we can calculate the elastic constants from the strain-stress

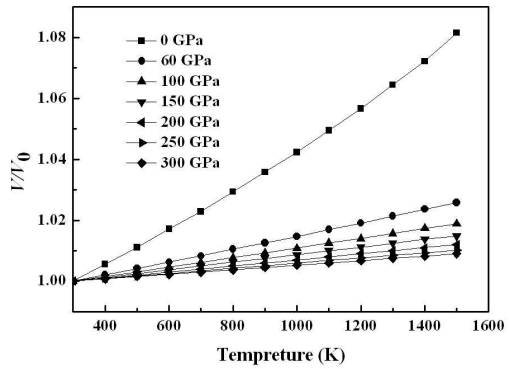

Figure 2: Isobars of the fcc Ni at different pressures.

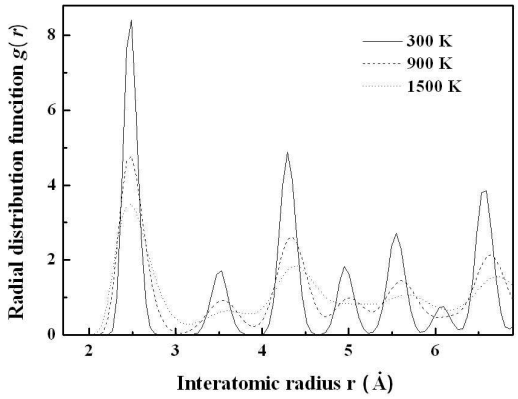

Figure 3: Calculated radial distribution function of Ni for: at $T=300$ K (solid line), at $T=900$ K (dashed line), at $T=1500$ K (dotted line).

relationships at the range of temperature from 300 K to 1300 K. In Table 1, the results of the calculations of the elastic constants and bulk modulus of Ni obtained from MD simulations are presented at 0 K and 300 K, compared with experiment [5] and other results [6,7]. For C_{44}, our result is as same as the experimental value, while Papanicolaou *et al.* [6] overestimates it by 12.0%. With C_{11} and C_{12}, our elastic constants are only 7.6%, 9.2% discrepancy with the experiment values, while Papanicolaou *et al.* continues to overestimate them by about 26.0%, 44.3%. At 300 K, our calculated results are in generally good accordance with the experimental and theoretical results [7] due to that the MD simulations fully include anharmonicity in the solid crystal.

According to the Vogit-Reuss-Hill approximation [34], we obtain the isotropic bulk modulus B_V and shear modulus G_V of a polycrystalline aggregate from the single-crystal elastic

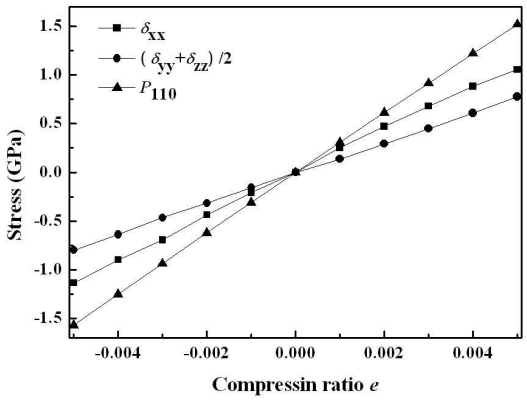

Figure 4: Stress as a function of compression ratio e, the elastic constant can be determined by the relations described in the text.

constants [19]

$$G_V = \frac{(C_{11}-C_{12}+3C_{44})}{5}, \tag{7}$$

$$G_R = \frac{5(C_{11}-C_{12})C_{44}}{\left(4C_{44}+3(C_{11}-C_{12})\right)}. \tag{8}$$

The arithmetic average of Voigt and Reuss bounds is called the Voigt-Reuss-Hill approximations [19]

$$G = \frac{(G_V+G_R)}{2}, \quad B = \frac{(C_{11}+2C_{12})}{3}. \tag{9}$$

The longitudinal, bulk, and shear sound velocities V_l, V_B and V_S can be given by

$$V_l = \left(\frac{(B+4/3G)}{\rho}\right)^{1/2}, \tag{10}$$

$$V_B = \left(\frac{B}{\rho}\right)^{1/2}, \tag{11}$$

$$V_S = \left(\frac{G}{\rho}\right)^{1/2}. \tag{12}$$

In Table 1, the temperature dependence of elastic constants, the bulk modulus B and the shear modulus G at zero pressure have been presented. It is clearly found that C_{11} is susceptible to the temperature, while C_{12} and C_{44} vary little under the effect of temperature. The elastic constant C_{11} represents elasticity in length. A longitudinal strain produces a change in C_{11}. The elastic constants C_{12} and C_{44} are related to the elasticity in shape, which is a shear constant. A transverse strain causes a change in shape without a change in volume. In Fig. 5, the variations of elastic constants with respect to temperature are given for Ni. The

Table 1: The elastic constants C_{ij}, the bulk modulus B, shear modulus G at high temperature T for Ni under temperature at zero pressure.

	T (K)	C_{11} (GPa)	C_{12} (GPa)	C_{44} (GPa)	B (GPa)	G (GPa)	B/G
Present	0	241.0	165.0	132.0	190.3	80.4	2.37
	100	232.0	164.0	125.0	186.7	74.5	2.50
	300	224.0	156.0	120.0	178.7	72.6	2.46
	500	207.0	142.0	112.0	163.7	68.4	2.39
	700	182.0	139.0	103.0	153.3	40.9	2.75
	900	172.0	125.0	96.0	140.7	54.9	2.55
	1100	159.0	115.0	91.0	129.7	51.9	2.50
	1300	152.0	100.0	83.0	117.4	52.2	2.24
Exp. [5]	0	261.0	151.0	132.0	190.3		
	300	243.6	149.4	119.6	186.7		
Ref. [6]	0	329.0	218.0	148.0	255.0		
Ref. [7]	300	252.7	167.7	116.3	196.1		

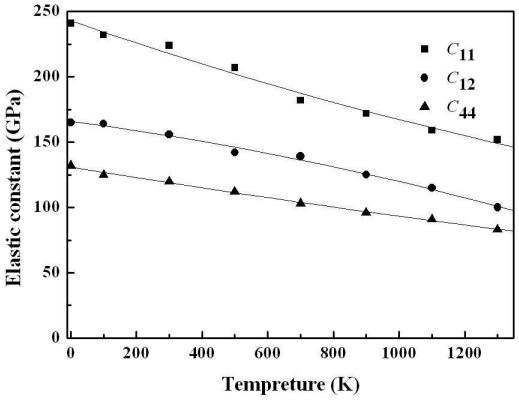

Figure 5: Elastic constants as functions of temperature at 0 GPa.

significant thermal softening in C_{11} is consequence of thermal expansivity. The bulk and shear modulus B and G as functions of temperature at ambient pressure are illustrated in Fig. 6. It is noted that with increasing temperature B and G decrease. For a cubic crystal, the mechanical stability leads to restrictions on the elastic constants as follows [35]: $C_{44}>0$, $C_{11}>|C_{12}|$ and $C_{11}+2C_{12}>0$. The elastic constants of Ni under temperature satisfy all of these conditions above. Therefore, Ni is mechanically stable at temperature up to 1300K.

Pugh [36] proposed the ratio of bulk to shear modulus, B/G, as an indication of ductile vs brittle characters. The bulk modulus B represents the resistance to fracture, while the shear modulus G represents the resistance to plastic deformation. A high B/G ratio is associated with ductility, whereas a low value corresponds to brittle nature. If $B/G>1.75$, the material behaves in a ductile manner; otherwise, the material behaves in a brittle manner. When the

applied temperature changes from 0 K to 1300 K, Ni is still a ductile material.

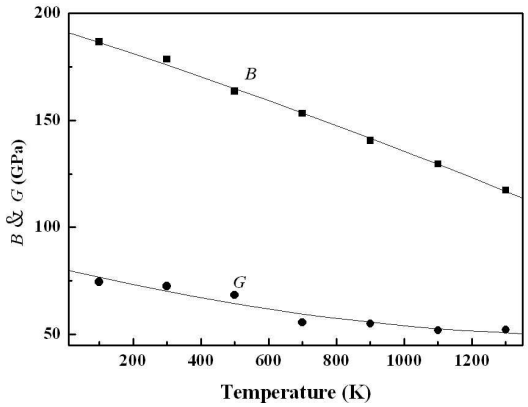

Figure 6: The bulk modulus B and shear modulus G as functions of temperature at ambient pressure.

In Fig. 7, we illustrate the calculated temperature dependencies of the longitudinal velocity V_l as well as the bulk velocity V_B and the shear sound velocities V_S. It is found that V_S, V_l and V_B decrease with increasing temperature, and this is because that vibration of atoms becomes more violent at higher temperature and the violent vibrations of atoms prevent the propagations of sound velocities.

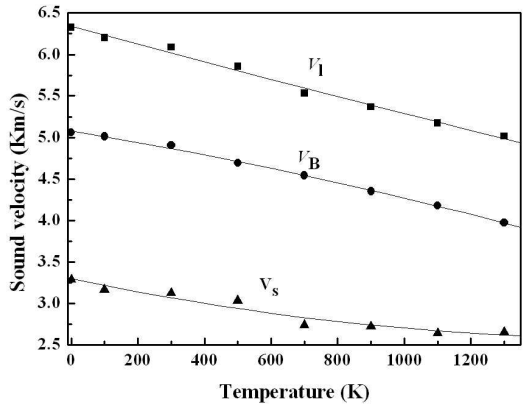

Figure 7: Sound velocities of Ni as a function of temperature at ambient pressure. The squares, circles and triangles represent the isotropic aggregate velocities V_l, V_B and V_S.

4 Summary

In summary, we have calculated the structures and the elastic constants of the fcc structured Ni at high temperature by using molecular dynamics with the direct method and the quantum

Sutton-Chen (Q-SC) potential. Our calculated elastic constants are in excellent agreement with available experimental data owing to anharmonic effects in the molecular dynamics. Our MD calculated results for the radial distribution function showed that the short-range atomic order of low-T is similar to the high-T solid, except that the coordination number of the first minimum is unchanged. The elastic constants, the bulk and shear modulus are presented. Moreover, from our elastic constants of Ni under temperature, we have found that Ni is ductile at high temperature, and is mechanically stable at temperature up to 1300 K.

Acknowledgments. The authors would like to thank the support by the National Natural Science Foundation of China under Grant No. 10776022 and the Specialized Research Fund for the Doctoral Program of Higher Education under Grant No. 20090181110080.

References

[1] W. Keim, Angew. Chem. Int. Ed. Engl. 29 (2003) 235.
[2] Y. M. Li, W. Y. Li, S. L. Chou, and J. Chen, J. Alloys Compd. 456 (2008) 339.
[3] S. Sivaprakash and S. B. Majumder, J. Alloys Compd. 479 (2009) 561.
[4] A. Dewaele, M. Torrent, P. Loubeyre, and M. Mezouar, Phys. Rev. B 78 (2008) 104102.
[5] G. Simmons and H. Wang, Single Crystal Elastic Constants and Calculated Aggregate Properties: A Handbook (M.I.T. Press, Cambridge, Massachusetts, 1971).
[6] N. I. Papanicolaou, H. Chamati, G. A. Evangelakis, and D. A. Papaconstantopoulos, Comput. Mater. Sci. 27 (2003) 191.
[7] S. Kamran, K. Y. Chen, and L. Chen, Phys. Rev. B 79 (2009) 024106.
[8] M. M. G. Alemany, O. Diéguez, C. Rey, and L. J. Gallego, Phys. Rev. B 60 (1999) 13.
[9] N. Jakse and A. Pasturel, J. Chem. Phys. 123 (2005) 244512.
[10] N. Jakse, J. F. Wax, and A. Pasturel, J. Chem. Phys. 126 (2007) 234508.
[11] P. Lazor, G. Shen, and S. K. Saxena, Phys. Chem. Miner. 20 (1993) 86.
[12] D. Errandonea, B. Schwager, R. Ditz, *et al.*, Phys. Rev. B 63 (2001) 132104.
[13] S. Japel, B. Schwager, R. Boehler, and M. Ross, Phys. Rev. Lett. 95 (2005) 167801.
[14] L. Kochi, E. M. Bringa, D. S. Ivanov, *et al.*, Phys. Rev. B 74 (2006) 012101.
[15] M. Ross, R. Boehler, and D. Errandonea, Phys. Rev. B 76 (2007) 184117.
[16] K. Kim, W. R. L. Lambrecht, and B. Segall, Phys. Rev. B 53 (1996) 16310.
[17] X. R. Chen, X. F. Li, L. C. Cai, and J. Zhu, Solid State Commun. 139 (2006) 249.
[18] P. Söderlind and J. A. Moriarty, Phys. Rev. B 57 (1998) 10340.
[19] O. Gülseren and R. E. Cohen, Phys. Rev. B 65 (2002) 06413.
[20] M. Parrinello and A. Rahman, J. Chem. Phys. 76 (1982) 2662.
[21] J. R. Ray, Comput. Phys. Rep. 8 (1988) 109.
[22] J. R. Ray and A. Rahman, J. Chem. Phys. 80 (1984) 4423.
[23] J. R. Ray and A. Rahman, J. Chem. Phys. 82 (1984) 4243.
[24] M. Sprik, R. W. Impey, and M. L. Klein, Phys. Rev. B 29 (1984) 4368.
[25] G. Gao, K. V. Workum, J. D. Schall, and J. A. Harrison, J. Phys.: Condens. Matter 18 (2006) S1737.
[26] J. D. Schall, G. Gao, and J. A. Harrison, Phys. Rev. B 77 (2008) 115209.
[27] Z. L. Liu, X. L. Zhang, L. C. Cai, *et al.*, J. Phys. Chem. Solids 69 (2008) 2833.
[28] T. Cagin, Y. Qi, H. Li, *et al.*, MRS Symp. Ser. 554 (1999) 43.
[29] W. G. Hoover, Phys. Rev. A 31 (1985) 1695.

[30] U. Essmann, L. Perera, M. L. Berkowitz, *et al.*, J. Chem. Phys. 103 (1995) 8577.
[31] W. Smith, T. R. Forrester, I. T. Todorov, and M. Leslie, The DL_POLY_2 User Manual, CCLRC Daresbury Laboratory (Daresbury, Warrington, United Kingdom, 2006).
[32] U. Essmann, L. Perea, M. L. Berkowitz, *et al.*, J. Chem. Phys. 81 (1984) 3684.
[33] W. B. Pearson, A Handbook of Lattice Spacings and Structures of Metals and Alloys (Pergamon, Oxford, 1967).
[34] R. W. Hill, Proc. Phys. Soc. 69 (1952) 518.
[35] G. V. Sin'ko and N. A. Smirnov, J. Phys.: Condens. Matter 14 (2002) 6989.
[36] S. F. Pugh, Philos. Mag. 45 (1954) 823.